

Characterizing the formability of mild steel in the production of square components by deep drawing process

Adnan I. Mohammed^{1*} 

¹ Production Engineering and Metallurgy Department, University of Technology, Baghdad, Iraq

* Corresponding author's e-mail: adnan.i.mohammed@uotechnology.edu.iq

ABSTRACT

The deep drawing process for square cups is commonly utilized in sheet metal forming. However, there are many associated defects, including fracture, earing, and wrinkling. A problem that has more attention in this work is the study of the influence of the different parameters, such as blank diameter, drawing speed, and punch profile radius, on the formability of the squared cups. Three circular blanks with diameters of 80, 90, and 100 mm, three punch profile radii of 4, 7, and 10 mm, and three drawing speeds of 100, 200, and 300 mm/min have been chosen, while the other parameters kept constant. The formability indicators utilized in this study are thickness distribution, maximum thinning and maximum drawing force. The experiments were designed according to L9 Taguchi method and analyzed by ANOVA and S/N ratios techniques. The results shown that square cup corners experience higher deformation than the side walls cup. Consequently, during plastic deformation, the metal flowing along the side walls of the cup is easier and more uniform than that in the corners. The best results were obtained using the 80 mm blank diameter, with 200 mm/min drawing speed, and 7 mm punch profile radius. This combination resulted in a uniform thickness distribution, a maximum thinning of 21%, and a maximum drawing force of 31.25 kN.

Keywords: formability, mild steel, square part, sheet metal forming, deep drawing.

INTRODUCTION

Deep drawing is a widely used industrial process for forming parts from sheet metals; it can produce very highly complex products. This technique is commonly utilized in the production of various parts, such as cans, automotive components, housings, and sinks, with its applications expanding continuously, as illustrated in Figure 1 [1–3]. In the deep drawing process, a sheet metal (blank) is drawn radially into the cavity of the die by the action of a punch. The blank is placed onto the die and a blank holder is then introduced on the upper surface of the blank to control the sliding of the blank during the forming process. When the punch goes down, it pushes the blank into the cavity of the die, and thus the blank takes the die shape [4–6]. Researchers conducted many studies to study the influence of process parameters on formability in the deep drawing. The

following literature review offers an overview of several main researches in this field.

Christine et al. [7] investigate how the deep drawing process is affected by changes in the blank holder force, along with different radii of the tool. Rajhi [8] conducts the numerical simulation by using ABAQUS software of the warm deep drawing process for producing an automotive oil sump made from Al 6061-T6 aluminum alloy, aiming at process optimization. Efforts were made by Jaber et al. [9] to enhance the formability of AISI 1006 steel alloy blanks during the deep drawing of square-shaped components. Sevskec et al. [10] provide thorough examination of deep drawing processes for cups made from steel alloy. Their research focuses on three key aspects: the sheet metal thinning, the ear height, and the maximum force values. Milek [11–13] focuses on experimentally determining the boundary conditions of material for computer simulations of deep drawing processes. Strengthening curves for different alloys were developed using

tensile tests. These experimentally derived material models have been implemented in ABAQUS software to simulate the deep drawing processes, with results validated against experimental results. The current research aims to investigate the effect of the process parameters in the conventional deep drawing to improve the formability of the squared cups. The formability indicators used in this study are maximum percentage thinning, thickness distribution, and drawing force [14–16].

EXPERIMENTAL PROCEDURES

Material selection

The properties of the material being drawn significantly affect the results of the drawing process. Mild steel alloy was selected for conducting the study. The used sheet has a thickness of 0.5mm, and the chemical composition analysis was performed in ALNABAA CO. Engineering Services using the spectrometer device (SPECTROMAXx, German, Ametek) to validate the manufacturing certificate of this alloy, as detailed in Table 1.

Tensile test

For determining the characteristics of the sheet metal (blank), samples underwent machining and testing in accordance with ASTM standard E8M specifications, as depicted in Figure 2 [12]. Tensile testing was conducted at a cross head velocity of 2 mm/min, with initial strain rate of 0.0007 s^{-1} , utilizing a WDW200E type tensile testing machine (class A). The mechanical properties for low carbon steel are outlined in Table 2.

Table 1. The chemical composition of 1008 mild steel

C %	Si %	Mn %	Cr %	Mo %	Cu %	Ti %	V %	S %	Ni %
0.08	0.003	0.31	0.021	< 0.005	> 0.052	0.008	0.002	0.037	0.077

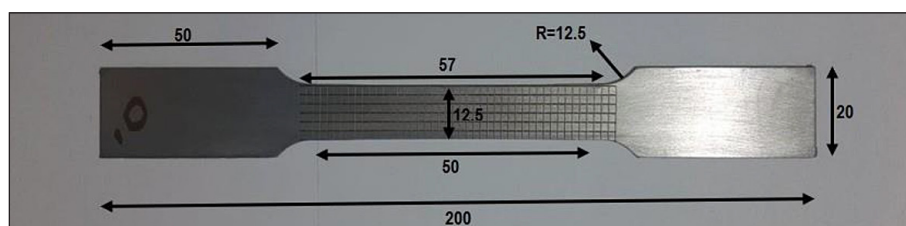


Figure 2. The standard specimen of tensile test according to ASTM E8M standard

Experimental tooling

The die and punch and were designed and machined to create square cups, as depicted in Figure 3. These tools have been manufactured from tool steel alloy, and have been machined by wire electric discharge machining (WEDM) machine, after machining, the tools have been polished to obtain better surface finish. The square punch measures 40 mm by 40 mm has corner radius of 5 mm, with profile radii of 4, 7, 10 mm each, resulting in a radial clearance of 0.55 mm when assembly with the die. The die with a flat surface features a square cavity measuring 41.1 mm by 41.1 mm, also having a die profile radius and corner radius of 5 mm.

Deep drawing test

The shape of blank used in this study was circular, with diameters $D = 80, 90, 100 \text{ mm}$. laser cutting is used to produce circular blanks, with a thickness of 0.5 mm each. The die has been positioned on a tensile machine with a capacity of 200 kN. Upon placing the blank on the surface of blank holder, the die descended towards the punch,

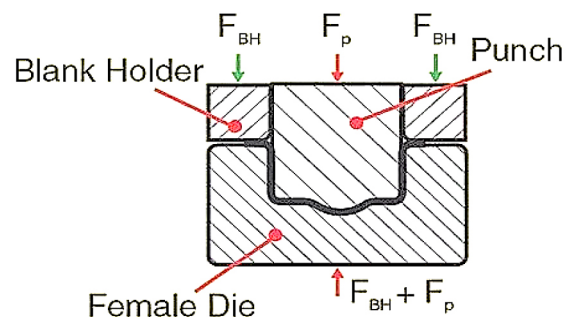


Figure 1. Conventional deep drawing process [4]

Table 2. The material properties of 1008AISI low carbon steel alloy

Yield strength, MPa	Ultimate tensile strength, MPa	Young modulus, MPa	Elongation at fracture, %	Reduction in area, %
218	366	200	21	37



Figure 3. The tool used in the study

indicating the use of an inverted drawing die. Various drawing speeds ranging from 100 to 300 mm/min were chosen for drawing the low carbon steel material. The blank holding force was determined through trial and error to be a minimum of 17 kN to prevent wrinkling during the deep drawing process. In order to study the thickness distribution within the cups during drawing operations, a grid pattern of 5, 10, 15, 20, 25, 30, 35, ... mm

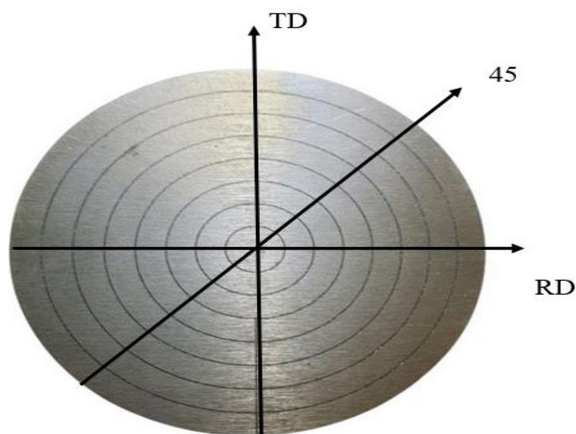


Figure 4. The blank surface was marked with a grid pattern

radii circles, was printed on undeformed blanks, by using a laser marking technique as shown in Figure 4. After drawing processes, the drawn cup was divided into two parts by using a wire electrical discharge machining (WEDM) as shown in Figure 5. A digital thickness micrometer with accuracy 0.001 mm is used to measure the cup wall thickness. Cup wall thickness is measured along the straight side (RD) from the bottom base center to the flange rim through interval 5 mm. While, the maximum force values have been recorded directly from the computer screen connected with tensile testing machine with a minimum measurement increment of 0.04 kN.

RESULTS AND DISCUSSION

In order to enhance the formability in the deep drawing process, the influence of the different parameters such as blank diameter, drawing speed and punch profile radius on the formability of the squared cups were studied. Three circular blanks with diameter 80, 90, 100 mm, three punch profile radius of 4, 7, 10 mm, and three drawing speed of

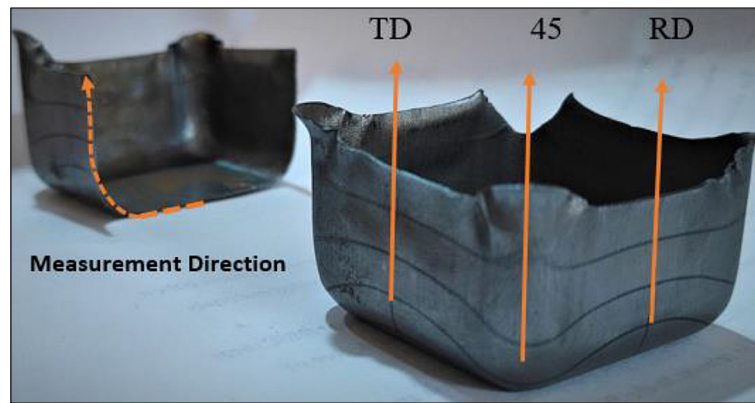


Figure 5. The indicated directions and path on the formed part in which the measurements were recorded

100, 100, 300 mm/min have been chosen, while the other parameters kept constant.

This paper is aimed to study the influence of process parameters on maximum thinning and maximum drawing force to enhance the quality of formed cups. First, the objective functions are defined, the process parameters are chosen, and an appropriate orthogonal array is built based on the degree of freedom of the factors. Subsequently, the experiments are performed for each set of process parameters designed using Taguchi orthogonal array. The experimental results are then transformed into Taguchi signal-to-noise (S/N) ratios to determine the optimal parameters. Analysis of variance (ANOVA) is performed to identify the significant parameters and their contribution. Finally, regression equations are formulated to explain the relationship between process parameters and outputs values. The Minitab program was used to design of experiments by using L9 Taguchi method. The objective function (lower is better) was selected in the cases (maximum thinning and maximum drawing force). The design of experiments and output values was designed as shown in Table 3.

S/N analysis

S/N ratio plot for maximum thinning

In the Taguchi method, the signal-to-noise S/N ratio is utilized to evaluate the deviation of the quality characteristic from its desired value. The signal refers to the desirable target value for good products (mean ratio), while the noise refers to the undesirable value (the standard deviation). There are three categories of quality characteristic analyzed using the S/N ratio: the-lower-the-better, the-higher-the-better, and the-nominal-the-better [13]. In this research, the maximum thinning is treated as the quality characteristic with the objective the-lower-the-better. The-lower-the-better criterion was selected as the lower thinning indicates higher thickness at the corner, and better formability. The S/N ratio plots for the maximum thinning observed at the corner of the part during the experiments are illustrated in Figure 6. These plots provide a visual representation of the effect of these parameters on maximum thinning, highlighting the optimal values for minimizing thinning along the cup wall. Based on the results,

Table 3. The design of experiments and output values

Blank diameter, mm	Speed, mm/min	Punch radius, mm	Maximum thinning, %	Maximum force, kN
80	100	4	22	32.32
80	200	7	21	31.25
80	300	10	23.6	34.01
90	100	7	24	32
90	200	10	37	33.03
90	300	4	27.5	36.3
100	100	10	38.2	39.9
100	200	4	32.2	43.8
100	300	7	32.8	35.7

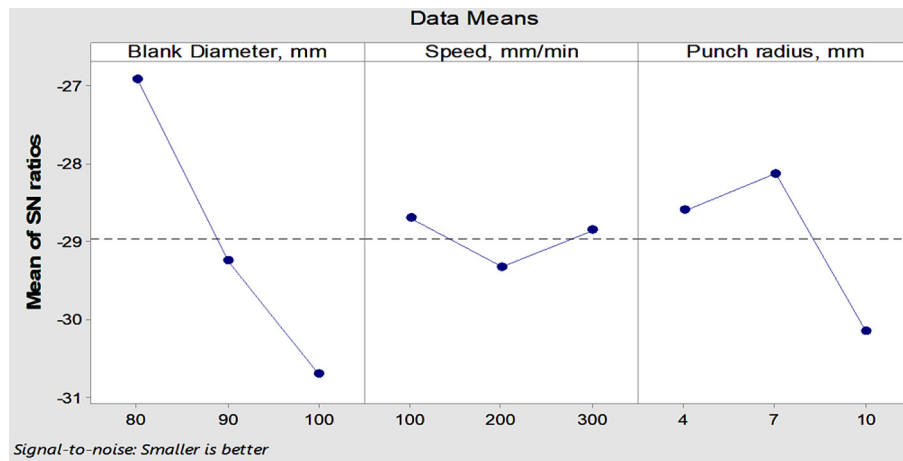


Figure 6. The S/N ratio plot for maximum thinning obtained from experimental results

the optimal combination of process parameters for minimizing the thinning in the deep drawing of square cup is obtained as (blank diameter of 80 mm, drawing speed 100 mm/min, punch profile radius of 7 mm). The S/N ratio values for the maximum thinning achieved experimentally at various levels of process parameters are also provided in Table 4. The term Delta refers to the total variation in mean thinning caused by changes in the level of individual process parameters. Among all the parameters, the process parameter (blank diameter) with the largest value of Delta was ranked one, indicating its the highest effect on the response (thinning). Punch radius was identified as the next influential parameter, ranked second, while the drawing speed was found the least influence among all the process parameters. The contribution of each parameter has been also worked out and these results are also illustrated in Table 4.

The obtained results indicated that increasing the blank diameter led to a rise in maximum thinning. This is attributed the higher force required to form larger diameter blanks. Notably, all experiments that failed were with blank diameter

equaled to 100 mm due to the excessive drawing ratio. This indicates that larger diameter of blank significantly challenge the sheet formability under the given process conditions. Furthermore, the influence of drawing speeds on maximum thinning was also studied. Increasing the drawing speed from 100 to 200 mm/min leads to increase in maximum thinning. This can be attributed by the increased strain hardening of the sheet at higher speeds, that limits its ability to deform evenly. However, when the drawing speed was further increased to 300 mm/min, the maximum thinning showed improvement, suggesting that given higher speeds may facilitate better metal flow and decrease localized thinning. The effect of punch radius on maximum thinning was also so important. Increasing the punch profile radius from 4 mm to 7 mm significantly reduce the maximum thinning along the cup wall, especially at the bottom corners. This improvement can be explained to the smoother transition of material flow over larger punch radius, which minimizes stress concentration. However, when the punch radius was further increased to 10 mm, wrinkling occurred. Results in restrain the flowing metal

Table 4. Response table for signal to noise ratios and contributions

Level	Blank diameter, mm	Speed, mm/min	Punch radius, mm	Error
1	-26.92	-28.70	-28.60	
2	-29.25	-29.32	-28.12	
3	-30.71	-28.85	-30.15	
Delta	3.79	0.62	2.03	
Rank	1	3	2	
SS	226.140	8.420	83.180	27.18
% Contribution	66.14	2.5	24.3	7.06

from flange region to die cavity region, ultimately leading to an increase in thinning again. These results underscore the significant of optimizing the punch radius to balance between avoid wrinkling and thinning. The thickness distribution curves corresponding to these observations are illustrated in Figure 7, providing a representation of how different process parameters affect thickness distribution during deep drawing process. These insights highlight the significant roles of blank diameter, punch profile radius, and drawing speed in achieving optimal distribution of thickness and minimizing thinning in the formed parts. Based on analysis of the experimental results using the Taguchi method, a regression equation for prediction the ‘maximum thinning’ was formulated in Equation 1. This equation estimates the maximum

thinning as a function of the process parameters within the specified range used in the paper.

$$\begin{aligned} \text{Maximum thinning} = & -32.8 + \\ & + 0.610 \text{ blank diameter} - 0.0005 \text{ speed} + \\ & + 0.950 \text{ punch radius} \end{aligned} \quad (1)$$

The S/N ratio plot for maximum drawing force

The smaller-the-better criterion has been selected for the response variable ‘maximum drawing force’ as lower forces result in reduced stresses along the cup wall, contributing to improved formability and quality of the final part. Figure 8 illustrates the S/N ratio plots for maximum force value obtained during the experiments. These graphs help visualize the effect of given process parameters on the drawing force and their

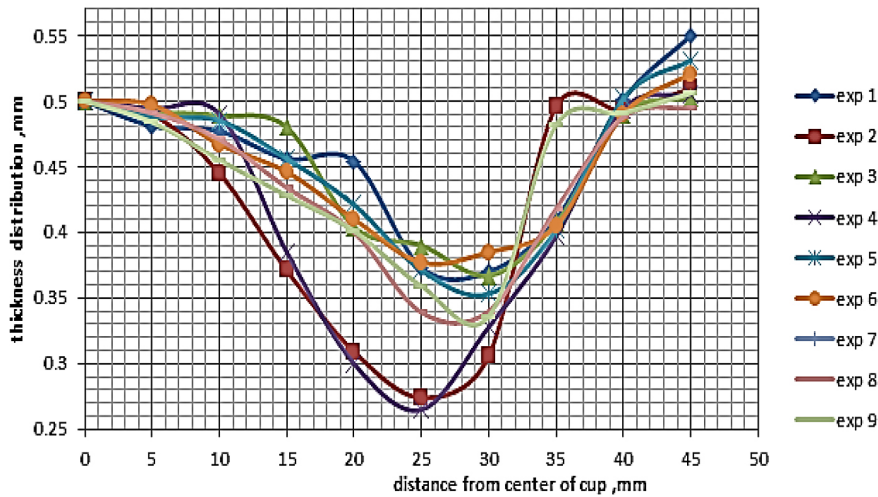


Figure 7. The thickness distribution curves for nine experiments

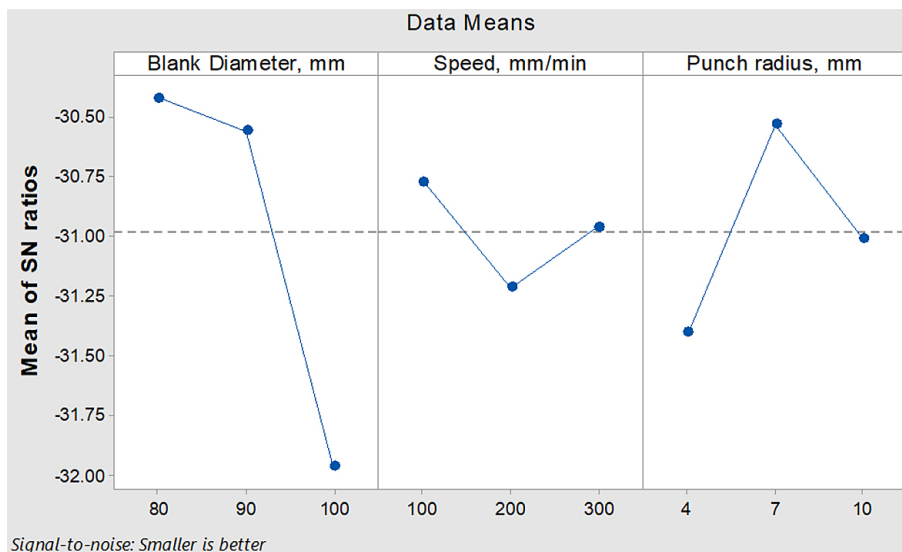


Figure 8. The S/N ratio plot for maximum force obtained from experimental results

Table 5. Response table for signal to noise ratios and contributions

Level	Blank diameter, mm	Speed, mm/min	Punch radius, mm	Error
1	-30.42	-30.77	-31.41	
2	-30.56	-31.21	-30.53	
3	-31.97	-30.96	-31.01	
Delta	1.55	0.44	0.87	
Rank	1	3	2	
SS	80.269	6.012	21.941	16.941
% Contribution	64.42	4.83	17.6	13.15

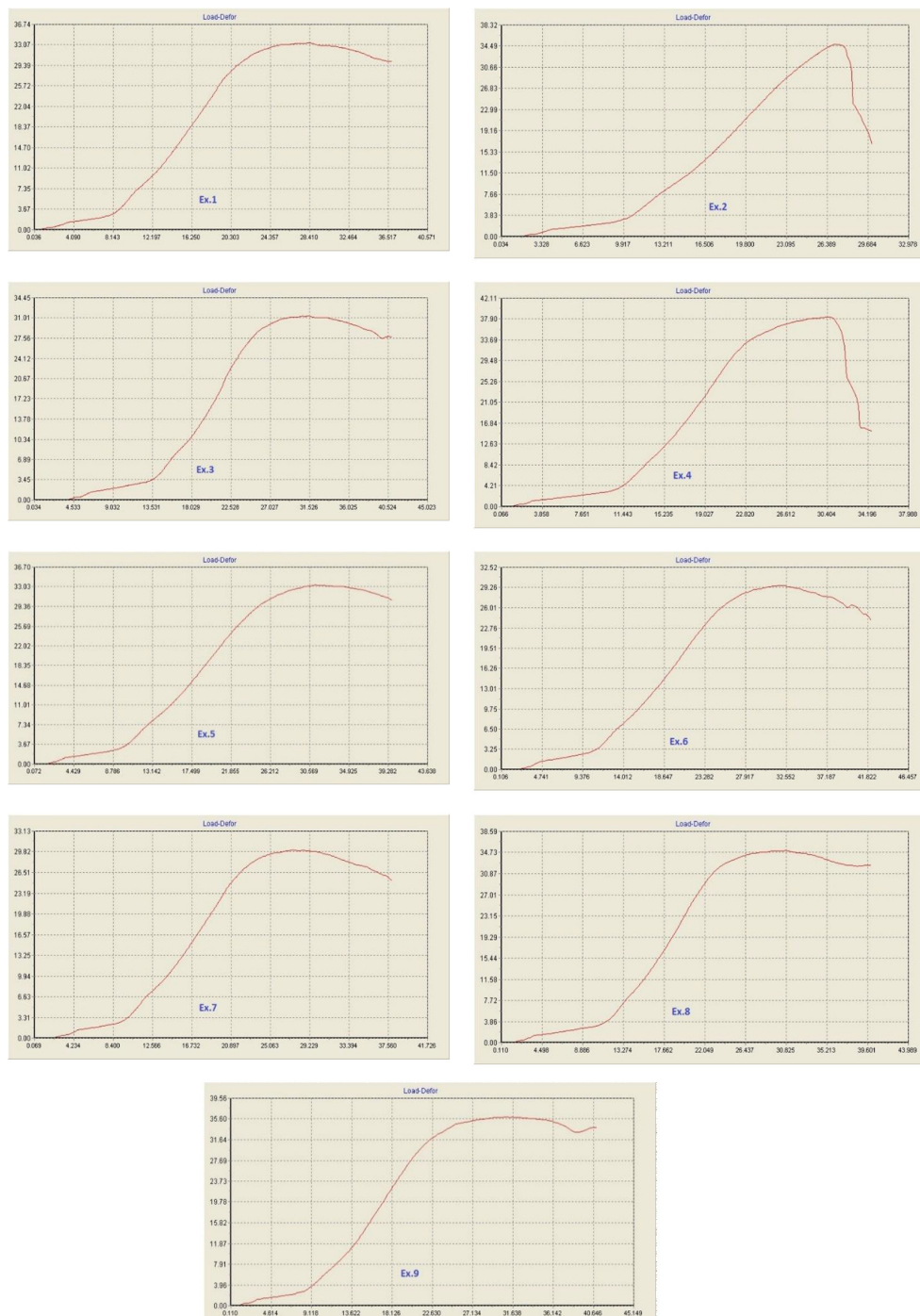


Figure 9. The load-displacement curves for nine experiments

contribution for minimizing stresses during the deep drawing process. The S/N ratio values for the experimentally achieved forces under various levels of process parameters are also presented in Table 5. Among the studied parameters, the process parameter (blank diameter) emerged as the most important factor effecting the drawing force. With the highest value of Delta value, it was ranked first. The second most influential parameter has been identified as the punch profile radius, ranked 2 in its effect on the maximum force. While, the drawing speed was found to have the least effect among all the parameters studied, ranking last. The detailed contributions of each parameter to the response variable are also summarized in Table 5.

The maximum drawing force increases clearly as the diameter of blank rises from 80 mm to 100 mm. This tendency shows that larger diameters lead to higher forces desired during the deep drawing process. Larger diameters lead to higher resistance because of increase in drawing area. Hence, reducing the blank diameter lowers the maximum force and improves the efficiency of forming process. The drawing force initially increase as the speed increases from 100 mm/min to 200 mm/min. However, the force slightly improves as the velocity increases further to 300 mm/min, pointing out a drop in the maximum force at higher speeds. This non-linear relation could be attributed to effects of strain rate. The force decreases significantly as the punch radius increases from 4 mm to 7 mm due to easier metal flow on larger radius. Where, Larger punch radius decreases concentrations of localized stress at the punch corners, allowing for smoother metal flow during deep drawing. However, further increasing the punch radius to 10 mm causes an increase in the drawing force. This could result from wrinkling or instability in the flange region due to excessive punch radii, which may prevent metal flow effectively. The load-deformation curves for all experiments is illustrated in Figure 9.

Based on the analysis of experimental results using the Taguchi method, a regression equation (Equation 2) was developed to estimate the maximum drawing force. This equation calculates the drawing force as a function of the given process parameters within the specified range considered in the research.

$$\begin{aligned} \text{Maximum force} = & 7.4 + \\ & + 0.330 \text{ blank diameter} + 0.0030 \text{ speed} - \\ & - 0.304 \text{ punch radius} \end{aligned} \quad (2)$$

CONCLUSIONS

Based on the results and discussion presented in this paper, the following conclusions are drawn:

1. Increase in the blank diameter increases the maximum force and maximum thinning, due to increase the amount of force required to form larger diameter. And all failed experiments were with blank diameter equaled to 100 mm.
2. Increasing the drawing speed from 100 to 200 mm/min leads to increase in maximum thinning. This can be attributed by the increased strain hardening of the sheet at higher speeds, that limits its ability to deform evenly. However, when the drawing speed was further increased to 300 mm/min, the maximum thinning showed improvement, suggesting that given higher speeds may facilitate better metal flow and decrease localized thinning.
3. Increase the punch profile radius from 4 mm to 7 mm reduce the maximum thinning along the cup wall especially, at corners. While, further increase of punch radius to 10 mm led to occurrence of wrinkling.
4. The best results have been obtained from the 80 mm blank diameter, with 200 mm/min drawing speed and 7 mm punch profile radius according to the uniform thickness distribution, lowest maximum thinning and lowest maximum drawing force.
5. The worst results have been obtained from the 100 mm blank diameter, with 200 mm/min drawing speed and 10 mm punch profile radius. This combination resulted in the highest thinning of 38.2%, and the maximum force of 39.9 kN, compared to the rest experiments conditions.

REFERENCES

1. Behrens B.-A., Hübner S., Wehmeyer J., Müller P., and Yarcu S. Tribological investigations of water-based lubricants for application in the deep drawing process, IOP Conf. Ser. Mater. Sci. Eng., 2024, 1307(1), 012001, <https://doi.org/10.1088/1757-899x/1307/1/012001>
2. Leng Y., Sanjon C. W., Tan Q., Groche P., Hauptmann M., and Majschak J. Study of Parameters Influencing Wrinkles in the Deep Drawing of Fiber-Based Materials Using Automatic Image Detection, 2024.
3. Xie H., Lu Y., Li R., and Liu J. Multi-pass deep-drawing process and mould design for thin-walled hollow cylindrical parts, Appl. Comput. Eng., 2024, 709(1), 85–91, <https://doi.org/10.1016/j.apcompe.2024.101085>

- org/10.54254/2755-2721/70/20240964
4. Heinzl C., Thiery S., and Khalifa B.N. Study on the effects of tool design and process parameters on the robustness of deep drawing, *Mater. Res. Proc.*, 2024, 41, 1488–1497, <https://doi.org/10.21741/9781644903131-165>
 5. Jaber A. S., Shukur J. J., and Khudhir W. S. Analysis of the process parameters effect on the thickness distribution and thinning ratio in single point incremental forming process, *J. Mech. Eng. Res. Dev.*, 2020, 43(7), 374–382.
 6. Shukur J. J. and Jaber A. S. Experimental and finite element analysis study of die geometrical affect the forming load during extrusion process, *IOP Conf. Ser. Mater. Sci. Eng.*, 2020, 881(1), <https://doi.org/10.1088/1757-899X/881/1/012045>
 7. Nizam M. Wrinkling Defect in Sheet Metal Process using Finite Element Analysis, *Int. J. Res. Appl. Sci. Eng. Technol.*, 2022, 10(6), 4421–4429, <https://doi.org/10.22214/ijras.2022.44947>
 8. Rajhi W. Numerical Simulation of Damage on Warm Deep Drawing of Al 6061-T6 Aluminium Alloy, *Eng. Technol. Appl. Sci. Res.*, 2019, 9(5), 4830–4834, <https://doi.org/10.48084/etasr.3148>
 9. Jaber A., Mohammed A., and Younis K. Improvement of Formability of AISI 1006 Sheets by Hydroforming with Die in Square Deep Drawing, *Eng. Technol. J.*, 2023, 0(0), 1–9, <https://doi.org/10.30684/etj.2023.141104.1482>
 10. Sevšek L., Vilkovský S., Majerníková J., and Pepelnjak T. Predicting the deep drawing process of TRIP steel grades using multilayer perceptron artificial neural networks, *Adv. Prod. Eng. Manag.*, 2024, 19(1), 46–64, <https://doi.org/10.14743/apem2024.1.492>
 11. Miłek T. Experimental determination of material boundary conditions for computer simulation of sheet metal deep drawing processes, *Adv. Sci. Technol. Res. J.*, 2023, 17(5), 360–373, <https://doi.org/10.12913/22998624/172364>
 12. ASTM, ASTM E8/E8M standard test methods for tension testing of metallic materials 1, *Annu. B. ASTM Stand.* 2010, 4,(I), C, 1–27, <https://doi.org/10.1520/E0008>
 13. Modi B. and Kumar D. R. Optimization of process parameters to enhance formability of AA 5182 alloy in deep drawing of square cups by hydroforming, *J. Mech. Sci. Technol.*, 2019, 33(11), 5337–5346, <https://doi.org/10.1007/s12206-019-1026-2>
 14. Bedan, A.S., Mansor, K.K., Anwer, K.K., Kadhim, H.H. Design and Implementation of Asymmetric Extrusion Die Using Bezier Technique, *IOP Conference Series: Materials Science and Engineering*, 2020, 881(1), 012052.
 15. Bedan, A.S., Shabeeb, A.H., Hussein, E.A. Improve single point incremental forming process performance using primary stretching forming process. *Advances in Science and Technology Research Journal*, 2023, 17(5), 260–268.
 16. Abbas, E.A., Mansor, K.K. Numerical and Experimental Investigation of the Effect of Strength of Aluminum 6061 Alloy on Thickness Reduction in Single-Point Incremental Forming, *Advances in Science and Technology Research Journal*, 2023, 17(4), 271–281.